Neuromol Med
DOI 10.1007/s12017-014-8315-9

ORIGINAL PAPER

The Aβ Peptides-Activated Calcium-Sensing Receptor Stimulates the Production and Secretion of Vascular Endothelial Growth Factor-A by Normoxic Adult Human Cortical Astrocytes

Ilaria Dal Prà · Ubaldo Armato · Franco Chioffi · Raffaella Pacchiana · James F. Whitfield · Balu Chakravarthy · Li Gui · Anna Chiarini

Received: 13 February 2014 / Accepted: 4 June 2014

Abstract The excess vascular endothelial growth factor (VEGF) produced in the Alzheimer's disease (AD) brain can harm neurons, blood vessels, and other components of the neurovascular units (NVUs). But could astrocytes partaking in networks of astrocyte-neuron teams and connected to blood vessels of NVUs contribute to VEGF production? We have shown with cultured cerebral cortical normal (i.e., untransformed) adult human astrocytes (NAHAs) that exogenous amyloid-β peptides (Aβs) stimulate the astrocytes to make and secrete large amounts of Aβs and nitric oxide by a mechanism mediated through the calcium-sensing receptor (CaSR). Here, we report that exogenous Aβs stimulate the NAHAs to produce and secrete even VEGF-A through a CaSR-mediated mechanism. This is indicated by the ability of Aβs to specifically bind the CaSR, and the capability of a CaSR activator, the "calcimimetic" NPS R-568, to imitate, and of the CaSR antagonist, "calcilytic" NPS 2143, to inhibit, the Aβs stimulation of VEGF-A production and secretion by the NAHAs. Thus, Aβs that accumulate in the AD brain may make the astrocytes that envelop and functionally collaborate with neurons into multi-agent AD-driving "machines" via a CaSR signaling mechanism(s). These observations suggest the possibility that CaSR allosteric antagonists such as NPS 2143 might impede AD progression.

Keywords Amyloid-β · Human adult · Astrocyte · Calcimimetic · Calcilytic · Calcium-sensing receptor · Vascular endothelial growth factor-A

Abbreviations

Aβ	Amyloid-β
Aβs	Aβ peptides
AD	Alzheimer's disease
BBB	Brain–blood barrier
CaSR	Calcium-sensing receptor
DMSO	Dimethyl sulfoxide
ERK	Extracellular signal-regulated kinase
fAβ	Fibrillary amyloid-β
HIF-1/2	Hypoxia-inducible element-1/2
HRE	Hypoxia-response element
ICW	In-cell Western
IDE	Insulin-degrading enzyme
NAHAs	Normal (untransformed) adult human astrocytes
NO	Nitric oxide
NVU	Neurovascular unit
PBS	Phosphate buffered saline
sAβ	Soluble amyloid-β
VEGF	Vascular endothelial growth factor

Electronic supplementary material The online version of this article (doi:10.1007/s12017-014-8315-9) contains supplementary material, which is available to authorized users.

I. Dal Prà (✉) · U. Armato · R. Pacchiana · A. Chiarini
Histology and Embryology Section, Department of Life and Reproduction Sciences, University of Verona Medical School, 8 Strada Le Grazie, 37134 Verona, Italy
e-mail: ippdalpra@gmail.com

F. Chioffi
Department of Neurology/Neurosurgery, St. Chiara Hospital, Largo Medaglie D'Oro 9, 38122 Trento, Italy

J. F. Whitfield · B. Chakravarthy
National Research Council of Canada, Montreal Road 51, Ottawa, ON K1A-0N6, Canada

L. Gui
Department of Neurology, Southwest Hospital, Third Military Medical University, Chongqing, China

Published online: 20 June 2014

Introduction

Vascular endothelial growth factor (VEGF)-A is a multifunctional cytokine first known for its roles in vasculogenesis and angiogenesis during prenatal and postnatal life (Carmeliet et al. 1996; Ferrara et al. 2003). VEGF activities are essential for embryo-fetal survival and normal development (Carmeliet et al. 1996). In the brain and retina, VEGF not only regulates angiogenesis but it also has roles in nonvascular activities in health and disease (Carmeliet and Storkebaum 2002). Among these is VEGF's promotion of the neurogenesis in the subgranular layer of the adult dentate *gyrus*, which supports hippocampal plasticity and cognitive functions, such as episodic memory encoding and retrieval, which progressively fail during Alzheimer's disease (AD) development (Carmeliet and Ruiz de Almodovar 2013). Moreover, VEGF-mediated hypoxic preconditioning protects animals from brain ischemic lesions (Wick et al. 2002). VEGF also favors the survival of spinal motoneurons after an excitotoxic exposure to glutamate and in animal models of amyotrophic lateral sclerosis (Tolosa et al. 2008). Besides these neuroprotective activities, VEGF is also a noxious factor in AD, multiple sclerosis, brain trauma, ischemia, and neuroinflammation, promoting neuronal death and brain–blood barrier (BBB) dysfunction (Merrill and Oldfield 2005; Carmeliet and Ruiz de Almodovar 2013). Immunoreactive VEGF was detected inside microglia, cerebrovascular endothelial cells, neurons, and activated astrocytes connected to blood microvessels walls via their end-feet and within diffuse perivascular $A\beta_{42}$ plaques in the neocortex of AD brains, but not of normal age-matched brains (Merrill and Oldfield 2005; Thirumangalakudi et al. 2006). Moreover, an upregulation of the *VEGF-A* gene is known to occur along with the accumulation of $A\beta_{42}$ in AD brains (Del Bo et al. 2009). In addition, a functional variant of the *VEGF* gene promoter coupled with elevated plasma levels of VEGF protein appears to increase the risk of accelerated AD progression, particularly in APOE-ε4-positive individuals (Del Bo et al. 2009).

As these lines of evidence indicate a link between VEGF overexpression and AD development, we looked for factors that would upregulate VEGF-A expression in our model system of cultured functionally normal phenotypically stable adult human cortical astrocytes (NAHAs). We had already reported that soluble or fibrillar $A\beta_{25\text{-}35}$, a widely used functional surrogate of $A\beta_{42}$ (Kaminsky et al. 2010), stimulated NAHAs to produce and secrete surpluses of $A\beta_{42}$ and VEGF-A (Chiarini et al. 2010; Armato et al. 2013b). We also had shown that NPS R-568, an allosteric agonist (i.e., a Ca^{2+} "imitator" or "calcimimetic") increasing the affinity of the calcium-sensing receptor (CaSR) for Ca^{2+} (Nemeth 2002; Ward and Riccardi 2012), stimulated the release of excess $A\beta_{42}$ and large amounts of nitric oxide (NO) from the same astrocytes (Armato et al. 2013a, b and unpublished results). Conversely, CaSR allosteric antagonists (i.e., "calcilytics") decreasing the affinity of CaSR for Ca^{2+} (Nemeth 2002; Ward and Riccardi 2012), specifically suppressed the Aβ•CaSR-driven surplus release of $A\beta_{42}$ and NO by the NAHAs (Dal Prà et al. 2005, 2014; Armato et al. 2013a, b). Notably, CaSR's expression is ubiquitous in the brain, in which it plays manifold physiological roles (Yano et al. 2004). The possible involvement of the CaSR in AD pathophysiology was suggested by finding that sAβ oligomers and fAβ aggregates bind and activate the CaSR because they, like other CaSR ligands such as polyamines, have regularly spaced arrays of positive charges (Ye et al. 1997; Conley et al. 2009; Nygaard and Strittmatter 2009; Armato et al. 2013a, b). Thus, a pathological Aβ•CaSR signaling inducing the neurotoxic release of compounds such as $A\beta_{42}$, NO, and perhaps VEGF by the large population of astrocytes enveloping and functionally collaborating with and controlling neurons as well as blood vessels may drive the progression of AD pathology. Therefore, we determined whether $A\beta_{25-35}$ and CaSR signaling together stimulated NAHAs to produce and secrete excess VEGF-A as well as we have shown them to stimulate NAHAs to make and secrete surplus $A\beta_{42}$ and NO (Dal Prà et al. 2005, 2011, 2014; Armato et al. 2013a, b).

Materials and Methods

Cell Cultures

Astrocytes were isolated from *left-over* surgical fragments of adult human temporal cortex provided by F.C., according to St. Chiara Hospital (Trento, Trentino, Italy) guidelines and with the written informed consent of all the patients and/or their next-of-kin. All the procedures were certified by the Joint Commission International (JCI), a branch of The Joint Commission USA (Oakbrook, IL; jcieurope@jcrinc.com), partnered in Italy with the Pro.Ge.A. *s.r.l.*, and accredited to the World Health Organization (WHO) as a nongovermental and nonprofit world leader organization evaluating health services and the safeguard of patients' rights on the basis of internationally shared quality standards. And the present research project has been given approval by the Ethical Committee of Verona's Integrated University-Hospital Institution.

Astrocytes were isolated by a mild treatment with 0.025 % (w/v) trypsin (Eurobio, Les Ulis Cedex, France) in Hank's Basal Salt Solution (BSS; Eurobio) followed by

trituration with Pasteur pipettes of decreasing bores. The released cells were planted in culture flasks (BD Biosciences, Le Pont de Claix, France) containing a medium made up of 89 % (v/v) of a 1:1 mixture of DMEM/F-12 medium (AppliChem GmbH, Darmstadt, Germany), 10 % (v/v) heat-inactivated (at 56 °C for 30 min) fetal bovine serum (FBS; BioWhittaker Europe SA, Verviers, Belgium), and 1 % (v/v) of a penicillin–streptomycin solution (Eurobio) and fibroblast growth factor-2 (10 ng ml^{-1}, Sigma, Milan Italy). This complete medium was replaced every 2–3 days. After reaching a 70 % confluence, the primary cells were detached with 0.025 % (v/v) trypsin and 0.02 % (w/v) EDTA (Eurobio) in Hank's BSS, split 1:4 and planted in new flasks. After the third subculture, a homogeneous population of astrocytes was obtained and fibroblast growth factor-2 supplementation was no longer required (Chiarini et al. 2010; Armato et al. 2013a). In these pure cultures, the astrocytes homogeneously expressed cell type-specific markers such as glial fibrillary acid protein (GFAP) and glutamine synthase (GS). None of the cultured cells expressed neuronal (enolase), oligodendrocytes (galactocerebroside), microglia (CD-68), or endothelial cells (factor VIII) markers. The adult astrocytes multiplied slowly in serum-enriched DMEM (AppliChem GmbH, Darmstadt, Germany). Proliferatively quiescent astrocytes in confluent cultures from the fourth to the eighth subculture were used for the present experiments.

Aβ Peptides and CaSR Agonists and Antagonists

$A\beta_{25–35}$ and $A\beta_{1–42}$ were from Bachem (Bubendorf, Switzerland). For the solubilization of $A\beta_{1–42}$, we first dissolved 4.5 mg of the peptide in 70 µl NH_4OH 1 % v/v solution (pH > 9) and next added 930 µl of phosphate buffered saline (PBS). This 1.0 mM solution was stored in small aliquots at −20 °C. To generate fibrils, 1.0 mM $A\beta_{1–42}$ aliquots were incubated for 5 days at 37 °C prior to be added to the growth media at a final $A\beta_{1–42}$ concentration of 5.0 µM. $A\beta_{25–35}$ peptides were dissolved at 1.5 mM in PBS. $A\beta_{25–35}$ fibrillogenesis took place within minutes at room temperature. Fibrillogenesis of Aβ peptides was checked via thioflavin-*T* tests before their experimental use (Dal Prà et al. 2011; Armato et al. 2013a; and unpublished data). Nonfibrillar $sA\beta_{25–35}$ was first dissolved at 4.0 mM in dimethyl sulfoxide (DMSO) (stock solution) and next directly diluted with the growth medium at final concentrations of 2–20 µM $sA\beta_{25–35}$ with 0.05–0.5 % DMSO, i.e., at DMSO concentrations previously reported to exert no noxious effects on nerve cells (Lu and Mattson 2001). The same amounts of DMSO were added in parallel to the growth media of corresponding untreated controls. The reversemer peptide $A\beta_{35–25}$ (Bachem) was dissolved in the same way as $A\beta_{25–35}$, but did not form fibrils.

The CaSR allosteric agonist ("calcimimetic") NPS R-568 (2-chloro-*N*-[(1*R*)-1-(3-methoxyphen-yl)ethyl]-benzenepropanamine hydrochloride; Tocris Bioscience, Bristol, UK) (Nemeth 2002) was prepared as a 100 mM stock solution in DMSO that was diluted into the growth medium at a final concentration of 1.0 µM in 1.0×10^{-5} % DMSO. This dose was maximally effective under the conditions used without being cytotoxic (Nemeth et al. 1998).

The CaSR allosteric antagonist ("calcilytic") NPS 2143 hydrochloride (2-chloro-6-[(2*R*)-3-[[1,1-dimethyl-2-(2-naphthalenyl)ethyl]-amino-2-hydroxypropoxy]-benzonitrile hydrochloride; Tocris Bioscience) (Nemeth 2002) was first prepared as stock solution (100 mM) in DMSO. This stock solution was diluted in the growth medium at a final concentration of 100 nM in 1.0×10^{-6} % DMSO. NPS 2143 has been shown to have an $IC_{50} = 43$ nM in HEK293 cells expressing the human CaSR (Nemeth 2002). Thus, the 100-nM dose we used was 2.33-fold the IC_{50} and under our conditions exerted a nearly maximal CaSR antagonistic effect with no concurrent cytotoxicity.

While experimenting with either agent corresponding amounts of DMSO were added to the growth media of the parallel controls.

Experimental Protocol

At experimental "0 h", some of the cultures served as untreated controls while others had 20 µM of either $fA\beta_{25–35}$ or reversemer $A\beta_{35–25}$ or 5.0 µM $fA\beta_{1–42}$ or various concentrations (range 2–20 µM) of $sA\beta_{25–35}$ added to their medium. The dose we used for the fAβs had been found to be optimal in previous studies (Ye et al. 1997; Nygaard and Strittmatter 2009; Dal Prà et al. 2011; Armato et al. 2013a).

Then again, when devised, starting at experimental "0 h" time and every 24 h thereafter astrocytes were first exposed for 30 min to either NPS 2143 (100 nM) or NPS R-568 (1.0 µM) dissolved in fresh medium prior to the adding of fAβs or sAβs; thereafter, we added to the cultures either fresh media (at 0.5 h) or the same media to which the astrocytes had been previously exposed (at both 24.5 and 48.5 h). Cultured astrocytes and their corresponding astrocytes-exposed media were sampled at 24 hourly intervals. Phosphoramidon (10 µM; Sigma Chemical Co., Milan, Italy), an inhibitor of thermolysin and other proteases, was added to the media at "0 h" experimental time.

Western Blotting (WB)

At selected time points, control and treated adult human astrocytes were scraped into cold PBS, sedimented at 200 × *g* for 10 min, and homogenized in T-PER™ tissue protein extraction reagent (Pierce-Celbio, Milan, Italy)

containing a complete EDTA-free protease inhibitor cocktail (Roche, Diagnostics, Milan, Italy). The protein contents of the samples were assayed via Bradford's protein assay kit (Bio-Rad, Milan, Italy) using bovine serum albumin as standard. Equal amounts (10–30 μg) of protein from the samples were heat-denatured for 10 min at 70 °C in an appropriate volume of 1x NuPAGE lithium dodecyl sulfate (LDS) Sample Buffer supplemented with 1x NuPAGE Reducing Agent (Invitrogen, Milan, Italy). The samples were next loaded on NuPAGE Novex 4–12 % Bis–Tris polyacrylamide gel (Invitrogen). After electrophoresis in NuPAGE 4-morpholine ethane sulfonic acid (MES) sodium dodecyl sulfate (SDS) Running Buffers using the Xcell SureLock^{TM} MiniCell (Invitrogen) (50 min runtime at 200 V constant), proteins were blotted onto nitrocellulose membranes (0.2 μm; Pall Life Sciences, Milan, Italy). To ensure efficient and reproducible binding to the membrane, transfer proceeded under low power conditions (30 V constant) for 1 h in 1x NuPAGE transfer buffer containing 10 % methanol. Immunoblots were performed using the SNAP i.d. protein detection system (Merck-Millipore, Milan, Italy) and the membranes were probed with (1) a specific rabbit polyclonal antibody against human VEGF-A (Santa Cruz Biotechnology, Heidelberg, Germany) at a final dilution of 1.0 μg ml^{-1}; (2) a monoclonal antibody against human CaSR HL1499 (Sigma) at a final dilution of 3.0 μg ml^{-1}; and (3) an antibody against lamin B1 (C-20, Santa Cruz) used at 1.0 μg ml^{-1} for the loading controls. Subsequent assessments of the specific bands integrated intensities were carried out using Sigmagel^{TM} software (Jandel Corp., Erkrath, Germany).

In-Cell Western (ICW) Assay of VEGF-A

Adult human astrocytes were grown in 24-well micro plates (cat- # 353847; BD Biosciences Discovery Labs, Milan, Italy) and treated for 72 h with sAβ_{25-35} (from 2.0 to 20 μM) alone or in conjunction with NPS 2143 (100 nM), according to the previously detailed *Experimental protocol* (see above). For each well, the medium was removed, and then 1.0 ml of fresh 4 % paraformaldehyde was added and incubated for 20 min at room temperature. The cells were permeabilized by washing five times in PBS buffer added with 0.5 % Triton X-100 for 5 min per wash on a shaker at room temperature, and next incubated in PBS/Odyssey blocking buffer (1:1; Li-Cor Biosciences, Lincoln, NE, USA) for 90 min on a shaker at room temperature. The blocking buffer was removed and replaced with a solution containing the primary antibody (anti-human VEGF-A IgG polyclonal antibody cat. # SC-152 clone A-20 from Santa Cruz, used in previous studies in which it had been validated via WBs using a blocking peptide (cat. # SC-152P, Santa Cruz)) (Chiarini et al. 2010) diluted 1:50 in PBS/Odyssey blocking buffer 1:1. On each plate, one well was incubated with Odyssey blocking buffer that did not contain primary antibody to serve as a negative control for the plate. The plates were incubated overnight at 4 °C on a shaker, then washed the following morning 5 times with PBS + 0.1 % Tween-20 for 5 min per wash at room temperature on a shaker. The cells were next incubated with the secondary goat-anti-rabbit-IgG antibody IRDye 800CW conjugate (Li-Cor Biosciences) diluted 1:800 in PBS/Odyssey blocking buffer 1:1 containing 0.2 % Tween-20 and the DNA stain TO-PRO-3 iodide (1:5,000, Invitrogen), which emits fluorescence at 700 nm and served to normalize the VEGF-A-related results in relation to well-to-well variations in the number of proliferatively quiescent astrocytes. For the control well, the solution contained only Odyssey blocking buffer in PBS 1:1, 0.2 % Tween-20 and the secondary antibody. The plates were incubated for 1 h at room temperature on a shaker, sheltered from light, then washed five times with PBS + 0.1 % Tween-20 for 5 min per wash at room temperature on a shaker while still sheltered from light. After removing the wash buffer, the plate was scanned an Odyssey^{TM} IR scanner and the results analyzed using the Image Studio^{TM} software (Li-Cor Biosciences). Results were expressed as relative VEGF-A amounts compared to those of the untreated control wells normalized as 1.0. In keeping with reports from other laboratories (Aguilar et al. 2010; Moerke and Hoffman 2011), the results of pilot experiments (not shown) had validated the full comparability between the findings gained via WB or ICW analysis. Since sAβs do not emit in the near infrared spectrum as instead fAβs do, using ICW analysis to assess sAβ_{25-35}'s effects reduced the astrocytes' numbers required while providing even higher degrees of sensitivity and precision (Aguilar et al. 2010).

ELISA Assays of Secreted VEGF-A

Growth media incubated with the astrocytes for 24 h were sampled at 0, and 24 h, 48, and 72 h after the onset of exposure to Aβ_{25-35} or Aβ_{1-42} with or without NPS 2143 added, or to NPS 2143 or to NPS R-568 alone or to reversemer Aβ_{35-25} by itself and next stored at −80 °C to be subsequently assayed for their VEGF-A content. This was done using a specific commercial ELISA kit (Peprotech EC, London, UK). The tests were carried out according to the instructions of the manufacturer. The sensitivity of the assays for VEGF-A was 16 pg ml^{-1}. Because the culture medium was fortified with FBS (10 % v/v), the bovine VEGF-A was also measured by the ELISA assay. Therefore, we always tested in parallel a sample of culture medium added with FBS (10 % v/v) that had never come in contact with the astrocytes (so called "negative control"). The

VEGF concentration of the negative controls was between 17 and 19 pg ml^{-1}. Therefore, the negative controls absorbance values of bovine VEGF-A were subtracted from the absorbance values of all the other corresponding medium samples that had been incubated with the astrocytes to attain the actual values of the VEGF-A released from the NAHAs.

ELISA for HIF-1α Transcriptional Activity

Nuclear proteins from treated and control astrocytes were extracted using a kit from Panomics (Fremont, CA, USA) as suggested by the manufacturer. Protein contents were assayed via Bradford's kit (Bio-Rad). An ELISA kit from Panomics was used to assess the hypoxia-response element (HRE) DNA binding of the nuclear-extracted HIF-1α (coupled with HIF-1β) transcription factor as previously described (Chiarini et al. 2010). Briefly, to form the HIF-1α•HRE DNA complexes, 40 µl of binding buffer master mix were incubated with 10 µl of sample nuclear extract (0.5 µg μl^{-1}) in the sample plates for 30 min at room temperature. From each well of the sample plate, 45 µl were then transferred to the assay plate. To capture the HIF-1α•HRE DNA complexes, the assay plates were washed thrice with the kit's buffer and the samples were incubated with a primary antibody against HIF-1α for 1 h at room temperature. After washing and incubation with the secondary antibody, colorimetric signals were then developed by adding a tetramethyl benzidine (TMB) substrate solution to each well and read with a Multiskan™ (Labsystems, Helsinki, Finland) spectrophotometer at 450 nm.

Statistical Analysis

SigmaStat 3.5™ Advisory Statistics for Scientists (Systat Software, Richmond, CA, USA) was used for data analysis. The WB-specific bands densitometric data were normalized to their loading control (lamin B1) band values and next analyzed by one-way ANOVA. When an F value was coupled with a $p \leq 0.05$, post hoc Holm–Sidak's test was used both for all pairwise comparisons and for comparisons versus corresponding control values and null hypotheses were rejected when $p > 0.05$.

Results

The stimulation of VEGF-A synthesis and secretion by NAHAs via $fA\beta_{25–35}$•CaSR or $fA\beta_{1–42}$•CaSR signaling is mimicked by "calcimimetic" NPS R-568 but fully suppressed by "calcilytic" NPS 2143

At the experimental "0" time, small amounts of VEGF-A were detected by WB analysis intracellularly and by ELISA assay in the growth media of the untreated NAHAs (Fig. 1a, b). A treatment between 0 and 72 h with $fA\beta_{25–35}$ (20 µM) alone did not increase the NAHAs' intracellular levels of VEGF-A (Fig. 1a, $p > 0.05$), as the intensified intracellular production of VEGF-A was masked by a steady loss of endogenous VEGF-A through its greatly increased (+200 %, $p < 0.001$) secretion into the growth medium (Fig. 1b; Table 1).

A mediation of this $fA\beta_{25–35}$-stimulation of VEGF-A production and secretion by an Aβ•CaSR-evoked signaling was indicated by five main sets of findings.

First

The Aβ peptides specifically and tightly bind to the CaSRs as shown by the results of current studies carried out by means of the in situ proximity ligation assay (*is*PLA) that allows to unambiguously image chosen protein–protein interactions (see Fig. 1S and technical details in Electronic Supplemental Data).

Second

A selective CaSR antagonist, the "calcilytic" NPS 2143, totally suppresses this $fA\beta_{25–35}$•CaSR-elicited VEGF-A overproduction without altering basal VEGF-A synthesis/secretion. Thus, adding NPS 2143 along with $fA\beta_{25–35}$ to the astrocytes' cultures causes the intracellular levels of VEGF-A to marginally drop by 24 and 48 h and then to slowly return to the starting value between 48 and 72 h (Fig. 1a, $p > 0.05$). NPS 2143 also totally suppresses $fA\beta_{25–35}$'s stimulation of VEGF-A secretion between 0 and 72 h (Fig. 1b, $p < 0.001$; Table 1). By itself, NPS 2143 did not significantly affect NAHAs' intracellular levels or secretion of VEGF-A (Fig. 1a, b, $p > 0.05$) indicating that it only targets CaSR's mediation of $fA\beta_{25–35}$ action (Armato et al. 2013a).

Third

If the CaSR signaling mediated the $fA\beta_{25–35}$ action on VEGF-A, then a CaSR activator such as the "calcimimetic" NPS R-568 should also stimulate VEGF-A production and secretion by the NAHAs. Indeed, NPS R-568 did marginally, though not significantly, increase the intracellular VEGF-A levels between 0 and 48 h (Fig. 1a, $p > 0.05$). However, the "calcimimetic" agent significantly increased (+65 %, $p < 0.001$) the amount of VEGF-A secreted between 0 and 72 h (Fig. 1b; Table 1).

Fourth

It remained to determine whether substituting $fA\beta_{1–42}$ for $fA\beta_{25–35}$ ± NPS 2143 provided functionally comparable

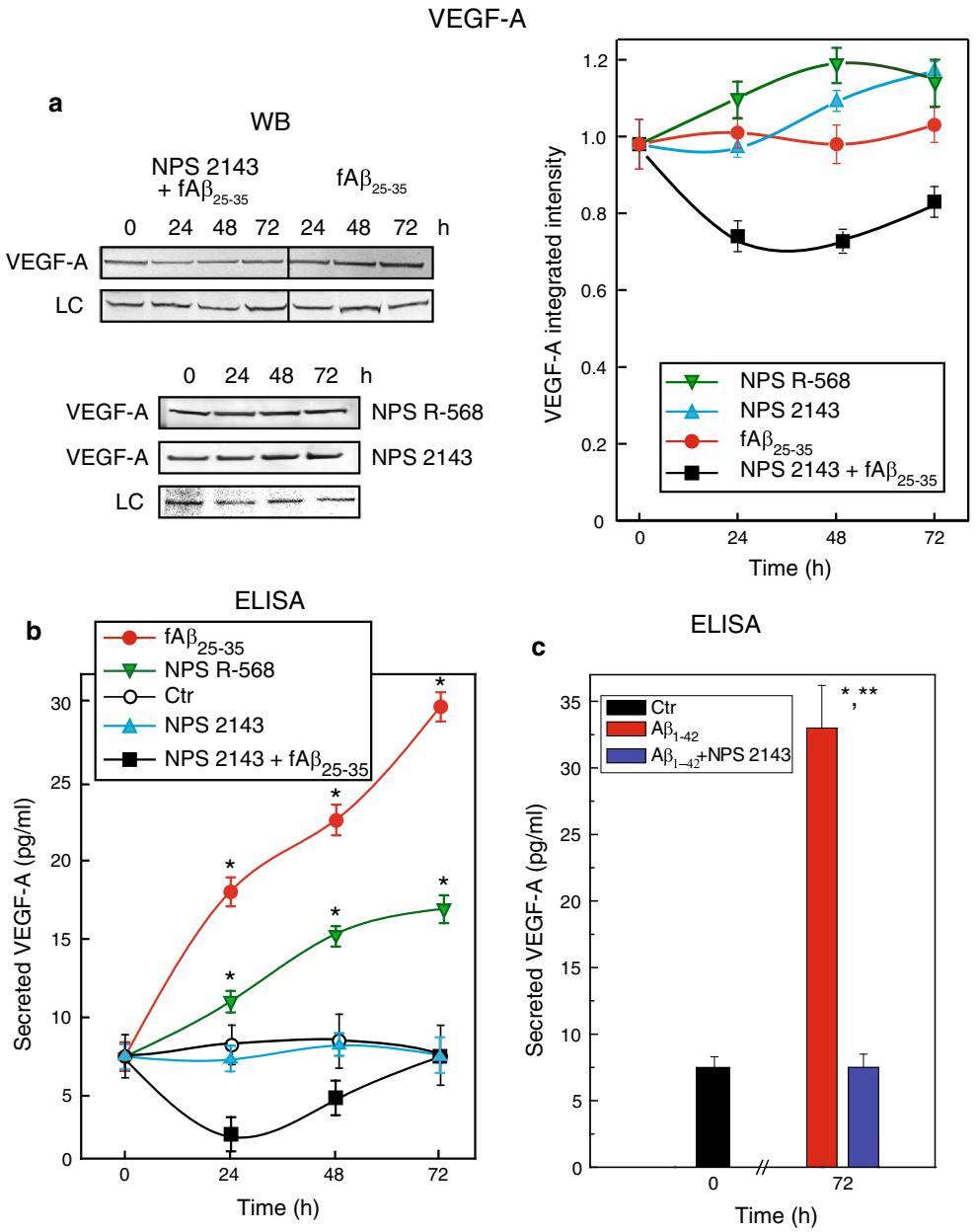

results. Thus, $fA\beta_{1-42}$ (5.0 μM) quadrupled ($p < 0.001$) by 72 h the amount of VEGF-A secreted by the NAHAs into their growth medium, an effect again totally suppressed by "calcilytic" NPS 2143 (Fig. 1c).

Fifth

Finally, the specificity of $fA\beta_{25-35}$'s CaSR-mediated actions on the NAHAs' VEGF-A metabolism was further proven by the total inability of the reversemer $A\beta_{35-25}$ to affect the astrocytes' VEGF-A production or secretion (not shown; see also Chiarini et al. 2010).

Also in keeping with our previous observations (Chiarini et al. 2010), an exposure of the NAHAs to $fA\beta_{25-35}$ was followed 18–24 h later by a surge of the intranuclear translocation of the HIF-1α•HIF-1β transcription factor and of its consequent binding to specific HRE DNA sequences (Fig. 2, $p < 0.05$ versus untreated controls). Conversely, "calcilytic" NPS 2143 prevented this $fA\beta_{25-35}$-induced HIF-1α•HIF-1β intranuclear translocation. During the first 18 h, the amount of intranuclearly translocated HIF-1α•HIF-1β transcription factor did not significantly drop below the starting value, but it did fall sharply and significantly ($p < 0.001$) between 18 and 24 h only to rise slowly toward but not to the starting value by 48 h (Fig. 2).

◀**Fig. 1** CaSR-mediated modulation of surplus VEGF-A synthesis and secretion in human adult cortical astrocytes. Cells were cultured, treated, and the biochemical assays of VEGF-A carried out as detailed in the Methods. **a** The astrocytes' intracellular levels of VEGF-A are not changed by each experimental treatment, though being insignificantly ($p = 0.06$) reduced by the NPS 2143 (100 nM) + $fA\beta_{25-35}$ (20 μM) treatment. *Left panel.* Typical immunoblots showing the specific bands pertaining to intracellular VEGF-A according to each treatment or to no treatment (i.e., experimental "0 h"). LC, loading control (lamin B1). *Right panel*. Densitometric evaluations of the whole sets of intracellular VEGF-A bands in the immunoblots for each time point and each treatment or no treatment. Points in the curves are the means ± SEM from 4 to 12 distinct experiments. ANOVA: treatment with *NPS R-568 (1.0 μM)*, $F = 1.494$, $p = 0.247$; treatment with *NPS 2143 (100 nM)*, $F = 1.048$, $p = 0.393$; treatment with *$fA\beta_{25-35}$ (20 μM)*, $F = 0.067$, $p = 0.977$; treatment with *$fA\beta_{25-35}$ (20 μM) + NPS 2143 (100 nM)*, $F = 2.969$, $p = 0.06$. **b** The secreted amounts of VEGF-A increase significantly after an exposure to $fA\beta_{25-35}$ (20 μM) alone or to "calcimimetic" NPS R-568 (1.0 μM); the $fA\beta_{25-35}$'s stimulatory effect is totally thwarted by NPS 2143 (100 nM), whereas the same NPS 2143 dose given by itself does not change the astrocytes' amounts of basally secreted VEGF-A. Points in the curves are the means ± SEM from 4 to 12 distinct experiments. *ANOVA:* untreated controls *(Ctr)*, $F = 0.945$, $p = 0.427$; treatment with *NPS 2143 (100 nM)*, $F = 0.659$, $p = 0.584$; treatment with *NPS R-568* (1.0 μM), $F = 24.412$, $p < 0.001$; post hoc Holm-Sidak's comparison test *versus* untreated controls, $^*p < 0.004$; treatment with *$fA\beta_{25-35}$ (20 μM)*, $F = 129.650$, $p < 0.001$; post hoc Holm-Sidak's comparison test *versus* untreated controls, $^*p < 0.001$; treatment with *$fA\beta_{25-35}$ (20 μM) + NPS 2143 (100 nM)*, $F = 2.699$, $p = 0.063$. **c** The amount of VEGF-A released from the astrocytes treated with $fA\beta_{1-42}$ (5.0 μM) significantly increases by 72 h just as it did with $fA\beta_{25-35}$ (20 μM) (cf. Fig. 1b), and this effect is fully suppressed by "calcilytic" NPS 2143 (100 nM). Points in the curves are the means ± SEM from 4 distinct experiments. *ANOVA:* treatment with *$fA\beta_{1-42}$ (5.0 μM)*, $F = 51.226$, $p < 0.001$; post hoc Holm-Sidak's pairwise comparison test: *$fA\beta_{1-42}$ (5.0 μM) versus* untreated controls, $^*p < 0.00001$; treatment with *$fA\beta_{1-42}$ (5.0 μM) alone versus $fA\beta_{1-42}$ (5.0 μM) + NPS 2143 (100 nM)*, $^{**}p < 0.00001$; treatment with *$fA\beta_{1-42}$ (5.0 μM) + NPS 2143 (100 nM) versus* untreated controls, $p = 0.953$

The stimulation of VEGF-A synthesis and secretion by NAHAs via $sA\beta_{25-35}$•CaSR or $sA\beta_{1-42}$•CaSR signaling is wholly suppressed by "calcilytic" NPS 2143

Next, we assessed the effects of 2.0–20 μM of $sA\beta_{25-35}$ on endogenous VEGF-A production and secretion by NAHAs. Thus, ELISA analysis showed that by 72-h daily doses of 10 or 20 μM $sA\beta_{25-35}$ stimulated VEGF-A secretion by 29 or 30 % (Fig. 3a, $p < 0.003$ and $p < 0.008$, respectively, versus untreated controls). On the other hand, ICW analysis revealed that by 72 h of daily administrations of 20 μM $sA\beta_{25-35}$ also correspondingly increased the intracellular VEGF-A level by 30 %, (Fig. 3b, $p < 0.004$ versus control values). Moreover, just as with $fA\beta_{25-35}$, "calcilytic" NPS 2143 totally suppressed the 20 μM $sA\beta_{25-35}$-elicited upsurge of VEGF-A intracellular accumulation and secretion (Fig. 3a, b).

Table 1 Total (0-to-72 h) VEGF-A secretion by adult human cortical astrocytes

Treatment	Total VEGF-A secreted[a]	% Change	Statistical significance[c]
None	816 ± 144[b]	–	–
NPS R-568	1,344 ± 99	+65	$p < 0.001$
$fA\beta_{25-35}$	2,448 ± 97	+200	$p < 0.001$
$fA\beta_{25-25}$ + NPS 2143	504 ± 100	−38 versus None	$p > 0.05$
		−79 versus $fA\beta_{25-25}$	$p < 0.001$
NPS 2143	759 ± 105	−7	$p > 0.05$

[a] The figures shown were obtained via the integral calculus of the surface areas (in mm^2) under the secretion curves in Fig. 1b

[b] Values are mean ± SEM from 4 to 12 distinct experiments

[c] One-way ANOVA analysis of the complete data set provided a value of $F = 114.970$, $p < 0.001$; pairwise comparisons were carried out using post hoc Holm–Sidak's test

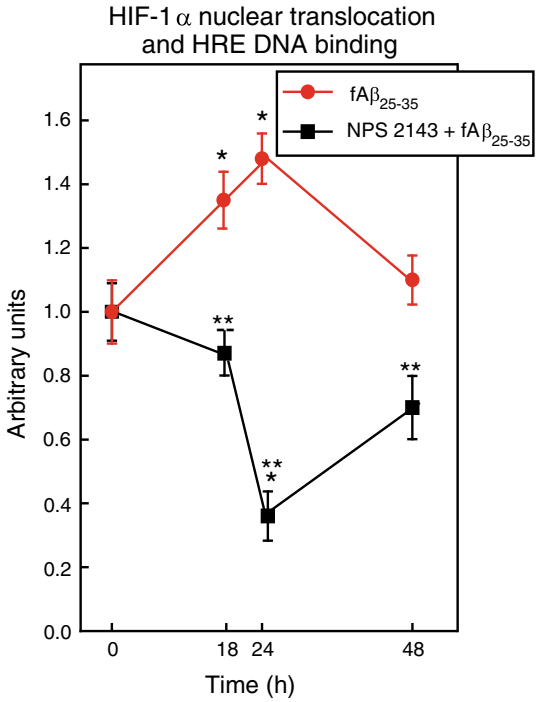

Fig. 2 $fA\beta_{25-35}$-enhanced nuclear translocation and HRE DNA binding of HIF-1α•HIF-1β transcription factor is significantly curbed by 24 h in astrocytes exposed to NPS 2143 (100 nM) + $fA\beta_{25-35}$ (20 μM). Points in the curves are the means ± SEM of 4 distinct experiments. *ANOVA:* treatment with *$fA\beta_{25-35}$ (20 μM)*, $F = 6.101$, $p < 0.006$; treatment with *$fA\beta_{25-35}$ (20 μM) + NPS 2143 (100 nM)*, $F = 9.720$, $p < 0.001$; comparisons of either treated group *versus* untreated controls with pairwise post hoc Holm-Sidak's test, $^*p < 0.05$; pairwise comparisons of corresponding time points of the two treatments with post hoc Holm-Sidak's test, $^{**}p < 0.0001$

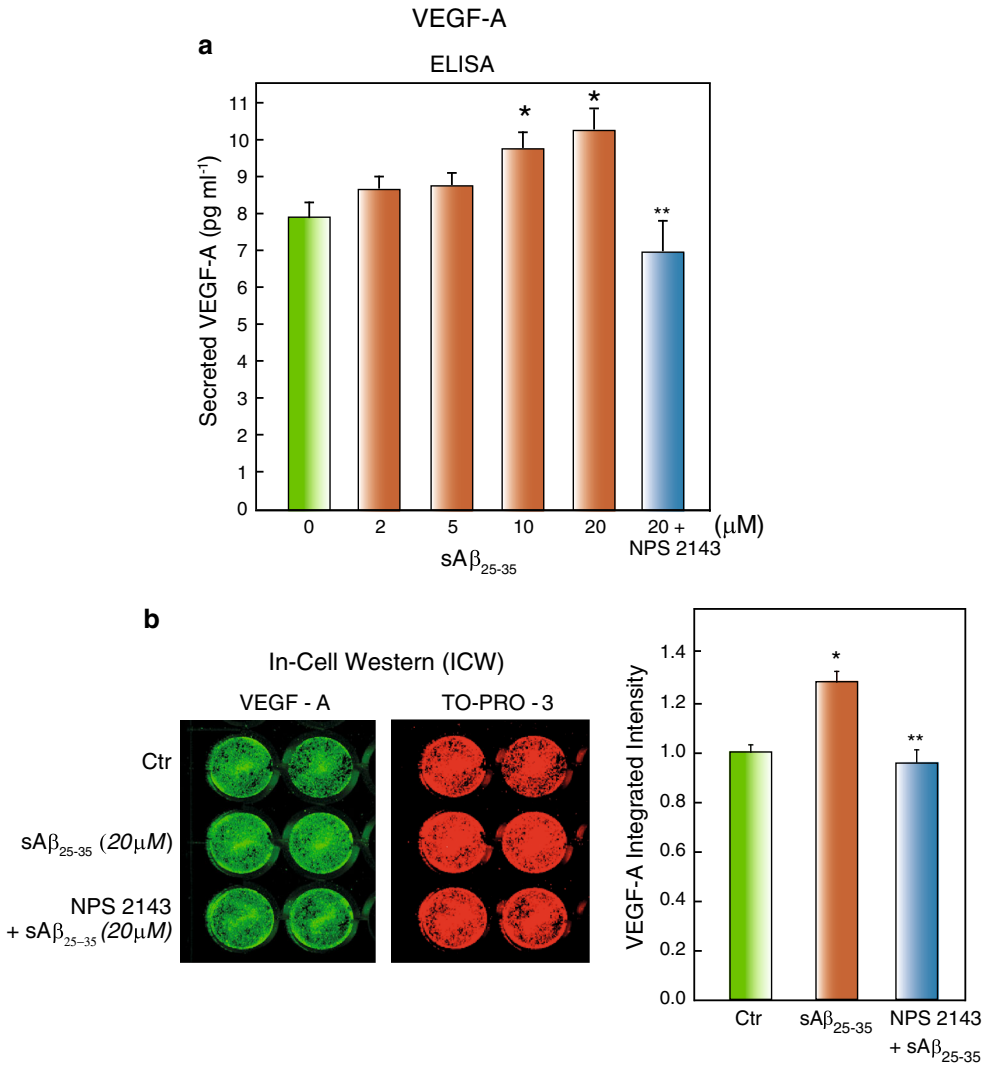

Fig. 3 Soluble (s) $A\beta_{25-35}$ triggers a less intense though significant VEGF-A upregulation than $fA\beta_{25-35}$ does in adult human cortical astrocytes, a stimulatory effect "calcilytic" NPS 2143 wholly curbs. **a** Dose-related effects of $sA\beta_{25-35}$ on the levels of secreted VEGF-A by adult human cortical astrocytes after deduction of the negative control medium data (see *Methods*). Only at concentrations $\geq$ 10 μM $sA\beta_{25-35}$ increases by 72 h the release of VEGF-A from the adult human cortical astrocytes and the 20 μM $sA\beta_{25-35}$'s effect is fully suppressed by NPS 2143. *ANOVA*. Treatment with $sA\beta_{25-35}$ *(2.0 μM)*, $F = 3.200$, $p = 0.124$; treatment with $sA\beta_{25-35}$ *(5.0 μM)*, $F = 5.000$, $p = 0.067$; treatment with $sA\beta_{25-35}$ *(10.0 μM)*, $F = 15.125$, $p = 0.008$; post hoc Holm-Sidak's comparison test *versus* untreated controls (Ctr), $^*p = 0.008$; treatment with $sA\beta_{25-35}$ *(20 μM)*, $F = 24.500$, $p = 0.003$; post hoc Holm-Sidak's comparison test *versus* Ctr, $^*p = 0.003$; and treatment with $sA\beta_{25-35}$ *(20 μM) + NPS 2143 (100 nM)*, $F = 4.500$, $p = 0.078$. **b** *Left panel*. Typical picture showing culture wells containing untreated or $sA\beta_{25-35}$ *(20 μM) ± NPS 2143 (100 nM)*-treated astrocytes, whose intracellular levels of VEGF-A underwent ICW analysis 72 h after the onset of the treatments. The astrocytes were doubly stained to simultaneously immunodetect their VEGF-A content (*green fluorescence*) and their DNA content (*red fluorescence* due to the DNA-bound TO-PRO-3 stain) as detailed in the *Methods*. The VEGF-A quantitative fluorescence data were normalized with the corresponding TO-PRO-3 data. *Right panel.* The TO-PRO-3-normalized integrated intensity results show a modest though significant increase in intracellular VEGF-A 72 h after a daily exposure to $sA\beta_{25-35}$ (20 μM) and its total suppression by NPS 2143 (100 nM). Bars are means ± SEM of 4 experiments each carried out in duplicate. *ANOVA*: treatment with $sA\beta_{25-35}$ *(20 μM)*, $F = 21.125$, $p = 0.004$; post hoc Holm-Sidak's comparison test *versus* untreated controls (Ctr), $^*p < 0.004$; treatment with $sA\beta_{25-35}$ *(20 μM) + NPS 2143 (100 nM)*, $F = 0.308$, $p = 0.599$

Discussion

In a normal human brain, astrocytes such as NAHAs may each envelop thousands of neuronal synapses with their mobile processes to form tripartite signaling teams. The astrocytes of these astrocyte-neuron teams also enwrap blood vessels with their end-feet that signal the blood vessels to widen and thus provide more blood and oxygen to support their teams' activities (Oberheim et al. 2009; Verkhratsky and Butt 2013). Our previous observations on

the cultured human NAHAs suggest that the Aβs accumulating in an AD brain once released from neurons stimulate their enveloping astrocytes to also make and secrete Aβs (Dal Prà et al. 2011, 2014; Armato et al. 2013a, b). Because of the large numbers and sizes of the teams' astrocytes' (Oberheim et al. 2009) they should substantially and increasingly contribute to the rising level of toxic Aβs in the brain (Armato et al. 2013a, b; Dal Prà et al. 2014).

Alterations in Ca^{2+}-regulating mechanisms at the cell surface and intracellularly have been previously suggested to occur in neurodegenerative disorders, AD included (Mattson et al. 1992; Mattson 2007; Berridge 2014).

The CaSR, a family C G-protein-coupled receptor, is expressed throughout the brain, where it has many physiological roles (Yano et al. 2004; Chakravarti et al. 2012). And the first hint of a possible involvement of the CaSR in AD pathophysiology was conveyed by its activation by the AD neuropathology-driving Aβ soluble oligomers and fibrillar aggregates (Ye et al. 1997) and later also by the findings of Dal Prà et al. (2005) and Conley et al. (2009). Recently, we showed that the Aβs interact with and persistently downregulate the CaSRs, the signaling of which mediates the astrocytes' ability to become neuron-killing machines that oversecrete the endogenously de novo synthesized Aβs and as well as make and secrete large amounts of NO and of the toxic peroxynitrite ($ONO\bar{O}$) derived from its interaction with reactive oxygen species (ROS) (Armato et al. 2013a, b; Dal Prà et al. 2014). Here, we have now shown that the Aβs specifically and tightly bind the CaSRs thereby also triggering an Aβ•CaSR signaling-induced stimulation of VEGF-A de novo production and secretion by the NAHAs.

Our conclusion that the Aβ•CaSR signaling mediates, besides endogenous Aβs oversecretion and NO excess production and release (Armato et al. 2013a, b), also VEGF surplus production and secretion is supported by the selective allosteric CaSR agonist ("calcimimetic") NPS R-568's stimulation of the NAHAs to make and secrete increased amounts of VEGF-A and by the suppression of the Aβ-raised VEGF production and secretion by the selective CaSR antagonist ("calcilytic") NPS 2143 (Nemeth et al. 1998, 2002).

The results of the present experiments on VEGF-A production and secretion by cultured NAHAs are very likely relevant to human AD because an increased production and secretion of VEGF-A by neurons, glia, and cerebrovascular endothelial cells is a feature of AD pathology: it exerts toxic effects on neurons and other constituents of the NVUs as well as causing BBB dysfunction (Sanchez et al. 2010, 2013; Davey et al. 2012; Ruhrberg and Bautch 2013). For example, the CaSR-mediated increase in the production of the potently angiogenic VEGF-A by Aβs-stimulated astrocytes would cause its overrelease from the end-feet of their blood vessels-enwrapping processes in hippocampal regions of the Aβs-accumulating brain. This could explain why functional magnetic resonance imaging (fMRI) reveals an unexpected supernormal blood oxygen level-dependent (BOLD) signaling from the task-responding, but already remarkably shrunken, dentate *gyrus*/CA3 hippocampal zones of mild cognitive impairment (MCI) brains (Dickerson et al. 2005; Ewers et al. 2011; Putcha et al. 2011; Yassa et al. 2010). The excess VEGF-A release could do this by increasing the blood vessel densities and thus blood oxygen deliveries in these regions when activated. This view is in keeping with the high capillary density associated with Aβ deposits found in the entorhinal cortex, hippocampus and subiculum of human AD brains as well as in the brains of APP23 AD-transgenic mice, and with the ability of microinjected $A\beta_{1-42}$ to stimulate angiogenesis in the rat hippocampus (Kawai et al. 1990; Logothetis and Wandell 2004; Zand et al. 2005). However, the supernormal hippocampal fMRI signaling eventually vanishes with the conversion from the mild cognitive impairment (MCI) stage to full blown AD probably because of the ultimate damage of blood vessels concurrently done by the progressively accumulating Aβs, proinflammatory cytokines, and NO (Myer et al. 2008; Chiarini et al. 2010; Jantaratnotai et al. 2011; Armato et al. 2013a).

As just said, the stimulation of VEGF-A's production and secretion by "calcimimetic" NPS R-568 (Nemeth 2002) supports a specific involvement of the CaSR in the process. On the other hand, "calcilytic" NPS 2143 only inhibited the fAβ•CaSR or sAβ•CaSR signaling that induced VEGF-A's surplus production and secretion but had no effect by itself. NPS 2143 similarly blocked the fAβ•CaSR- or sAβ•CaSR-stimulated excess secretion of endogenous $A\beta_{42}$ but did not affect basal $A\beta_{42}$ secretion when given alone (Armato et al. 2013a).

The reasons for these different effects of the CaSR antagonist are not understood. The many signaling pathways the CaSR activates include several second messenger-relaying enzymes (e.g, adenylyl cyclase), lipid kinases (e.g, phospholipase A2, C, D,), protein kinases (e.g, protein kinase Cs, mitogen-activated protein kinases, Akt/protein kinase B) as well as TRPC6-encoded receptor-operated

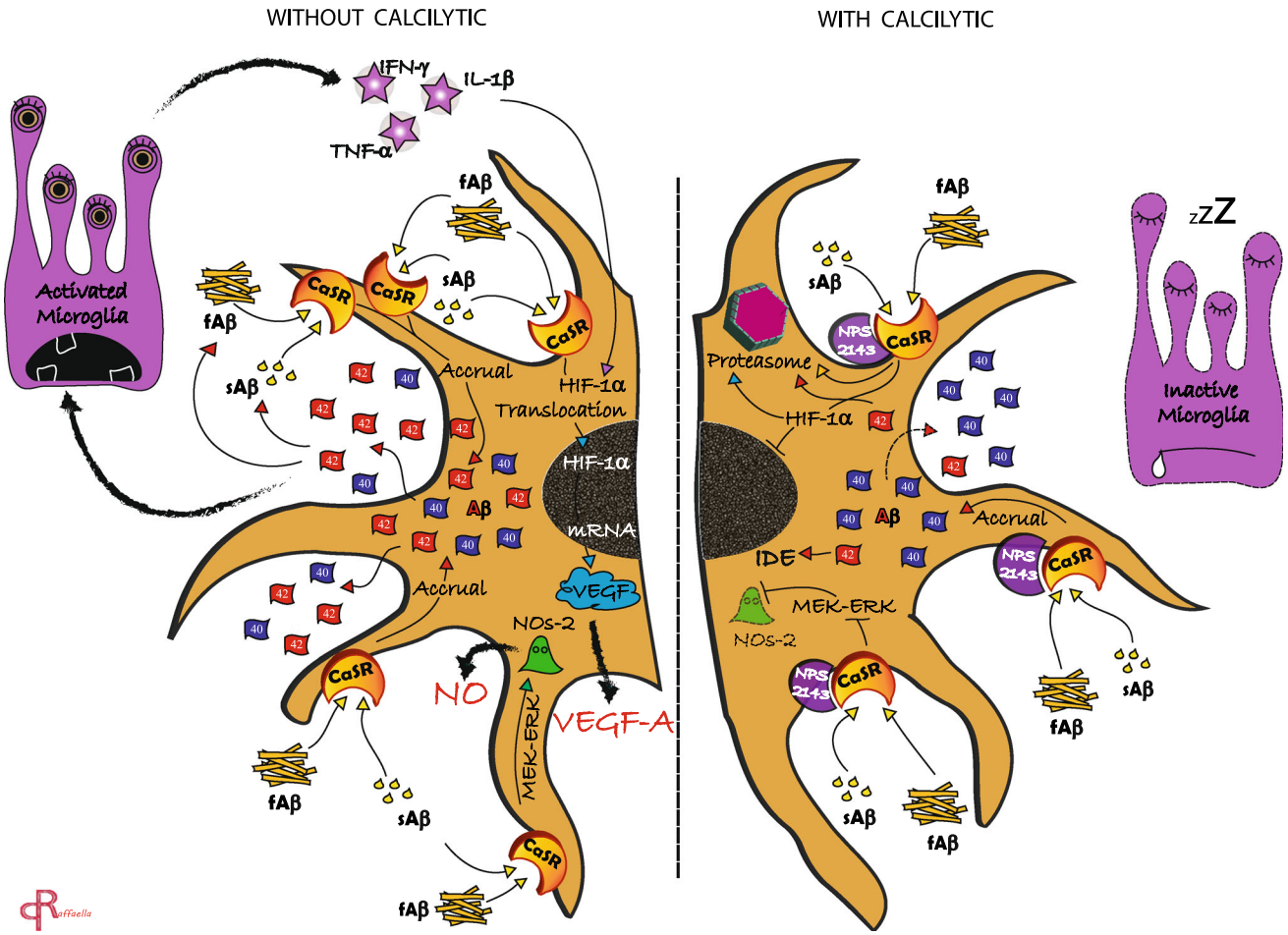

Ca^{2+} channels, and transcription factors (reviewed in Chakravarti et al. 2012). Hence, complex probably reciprocally cross-talking mechanisms are triggered not only by Ca^{2+}-activated CaSRs but also by CaSRs activated by the fAβs or sAβs. Like other GPCRs, CaSR displays a "*ligand-biased signaling*", by which a particular CaSR-stimulated pathway may be preferred over the others according to the activating ligand. This feature can be induced even by CaSR's allosteric agonists or antagonists (Davey et al. 2012; Leach et al. 2013). Moreover, the picture is made even more complex by changes in the total amount of available CaSR. In the NAHAs, the total CaSR level was found to be transiently increased (peak at 48 h) by $fA\beta_{25–35}$ alone, unaffected by the "calcimimetic" NPS R-568, and slightly but transiently reduced by "calcilytic" NPS 2143 given by itself. But the CaSR level was quickly, remarkably, and steadily downregulated by NPS 2143 plus $fA\beta_{25–35}$ (Armato et al. 2013a). It seems likely that this steep drop of the Aβ-bound CaSR and consequently its intracellular signaling is one of the reasons why NPS 2143 inhibited the production and secretion of VEGF-A by NAHAs in the present study as well as the secretion by NAHAs of the exogenously induced endogenous $A\beta_{42}$ in our previous study (Armato et al. 2013a). Interestingly, this NPS 2143 inhibition of Aβ•CaSR signaling was also accompanied by a sharp surge of proteasomal chymotrypsin-like (20S) activity peaking by 24 h and then dropping (Armato et al. 2013a). Such a surge of 20S proteasomal activity may have contributed to the observed destabilization and decreased availability of the VEGF-A gene's HIF-1α•HIF-1β transcription factor that would account for the NPS 2341 inhibition of Aβs-induced VEGF-A production and secretion.

In summary (Fig. 4), the present findings add another AD-participant, VEGF-A, to the previously identified endogenous $A\beta_{42}$ and NO induced by exogenous Aβ•CaSR interactions (Armato et al. 2013a, b). The mediation of the induction of these components of AD pathology in the astrocytes by the CaSR and the availability of potent selective CaSR blockers, such as the "calcilytic" NPS 2143, offer a possible way to at least impede the development of AD pathology.

◀**Fig. 4** "Calcilytic" NPS 2143 preserves normal physiological conditions in adult human cortical astrocytes exposed to fAβs and/or sAβs. *Left panel*. An aging-linked slowing of the $A\beta_{42}$ brain clearance is believed to start a progressive extracellular accrual first of soluble oligomeric $A\beta_{42}$ (*sAβ*) and later of fibrillar polymeric $A\beta_{42}$ (*fAβ*). The accumulating sAβs and fAβs interact with the CaSRs located at the plasma membrane of the depicted astrocyte's left half (Armato et al. 2013a, b). The fAβ•CaSR or sAβ•CaSR signaling elicits a set of harmful metabolic effects that start self-maintaining and further spreading vicious cycles. *First*. The production and intracellular accrual of endogenous $A\beta_{42}$ and $A\beta_{40}$ is significantly raised together with a surge in the secretion of exclusively $A\beta_{42}$ (Armato et al. 2013a, b), which diffuses in the extracellular environment and hence furthers its own production and secretion from neighboring astrocyte-neuron teams (*not shown*). *Second*. An Aβ•CaSR signaling-triggered, MEK/ERK-mediated surplus production and release of NO by inducible NO synthase-2 (depicted as a *wee ghost*) is evoked that (1) inhibits insulin-degrading enzyme (IDE)'s activity thereby favoring $A\beta_{42}$ accrual, and (2) nitrosylates critical functional components of the cells (*not shown*) (Dal Prà et al. 2005; Armato et al. 2013a). *Third*. An Aβ•CaSR signaling-elicited stabilization and intranuclear translocation of the HIF-1α•HIF-1β transcription factor interacting with DNA HREs of the *VEGF-A* gene increases the synthesis coupled with the prompt release of huge amounts of VEGF-A, in parallel with the overreleases of $A\beta_{42}$ and NO; ultimately, this excess VEGF-A harms the NVUs cellular components, alters BBB's permeability, worsens the brain tissue hypoperfusion, and exerts various toxic effects on the neurons advancing their demise (*not shown*) (Sanchez et al. 2013). *Fourth.* The accrued extracellular $A\beta_{42}$ oligomers and fibrils activate the microglia (depicted as a "*multi-eyed hydra"*), which then release, besides harmful reactive oxygen species (ROS), an array of proinflammatory cytokines that act synergistically with $A\beta_{42}$ to drive an additional surplus production and release of Aβs, NO, and particularly VEGF-A from the activated astrocytes (Blasko et al. 2000; Dal Prà et al. 2005; Chiarini et al. 2010; Armato et al. 2013a) resulting in an intensification of the toxic effects on neurons and of BBB's dysfunction (*not shown*) (Sanchez et al. 2013). *Right panel*. Adding the allosteric CaSR antagonist ("calcilytic") NPS 2143 prevents any such harmful occurrence by keeping the just detailed various metabolic processes within their physiological limits notwithstanding an initial extracellular accrual of sAβs and/or fAβs. *First*. The Aβ•CaSR complexes are markedly downregulated thereby desensitizing the astrocyte from the consequences of their enhanced signaling (Armato et al. 2013a). *Second.* The Aβ•CaSR signaling-induced intracellular accrual of endogenous $A\beta_{42}$ is effectively removed by a transiently increased activity of the 20S proteasomal chymotrypsin-like activity, the activation of various $A\beta_{42}$-cleaving proteases, including neprilysin, and the lack of NO-elicited IDE inhibition (see also *Fourth*) (Armato et al. 2013a, b). *Third.* The amount of secreted $A\beta_{42}$ is brought back to physiological, i.e., beneficial levels, whereas the release of $A\beta_{40}$ is lightly increased: these combined effects restore the extracellular $A\beta_{42}/A\beta_{40}$ ratio values to normal (*not shown*) (Armato et al. 2013a). *Fourth*. The Aβ•CaSR-evoked activation of the MEK/ERK pathway leading to an overproduction of tetrahydrobiopterin (BH4) necessary for the activation of inducible NO synthase (NOS)-2 (here drawn as a *vanishing "ghost"*) and IDE-inhibiting excess NO production and release is effectively prevented (Dal Prà et al. 2005; Armato et al. 2013a, b). *Fifth.* The cytoplasmic HIF-1α•HIF-1β transcription factors are destabilized and destroyed in the proteasome thereby preventing their intranuclear translocation and interaction with DNA HRE sequences; hence, *VEGF-A* gene expression is not increased, and VEGF-A proteins production and release stay at their physiological levels (Chiarini et al. 2010, and present results), which safeguards neurons' viability and BBB's normal functioning. *Sixth*. Microglia remains in a quiescent condition (here suggested by the *hydra's closed eyes*) as no progressive extracellular $A\beta_{42}$ accrual occurs: hence, the several proinflammatory cytokines are not oversecreted and none of their noxious effects obtains (Ryu and McLarnon 2009)

Acknowledgments This work was supported in part by the Italian Ministry for University and Research (ex-60 % Funds to UA, AC, and IDP).

Conflict of interest All authors declare that they have no conflict of interest.

Ethics standard The authors declare that the manuscript does not contain clinical studies or patient data.

References

Aguilar, H. N., Zielnik, B., Tracey, C. N., & Mitchell, B. F. (2010). Quantification of rapid myosin regulatory light chain phosphorylation using high-throughput in-cell Western assays: Comparison to Western immunoblots. *PLoS One, 5*(4), e9965.

Armato, U., Bonafini, C., Chakravarthy, B., Pacchiana, C., Chiarini, A., Whitfield, J. F., et al. (2012). The calcium-sensing receptor: A novel Alzheimer's disease crucial target? *Journal of Neurological Sciences, 322*(1–2), 137–140.

Armato, U., Chakravarthy, B., Pacchiana, R., & Whitfield, J. F. (2013a). Alzheimer's disease: An update of the roles of receptors, astrocytes and primary cilia (review). *International Journal of Molecular Medicine, 31*(1), 3–10.

Armato, U., Chiarini, A., Chakravarthy, B., Chioffi, F., Pacchiana, R., Colarusso, E., et al. (2013b). Calcium-sensing receptor antagonist (calcilytic) NPS 2143 specifically block the increased secretion of endogenous Aβ42 prompted by exogenous fibrillary or soluble Aβ25-35 in human cortical astrocytes and neurons—Therapeutic relevance to Alzheimer's disease. *Biochimica et Biophysica Acta, 1832*(10), 1634–1652.

Berridge, M. J. (2014). Calcium regulation of neural rhythms, memory and Alzheimer's disease. *Journal of Physiology, 592*(Pt 2), 281–293.

Blasko, I., Veerhuis, R., Stampfer-Koutchev, M., Sauerwein-Teissl, M., Eikelenboom, P., & Grubeck-Loebenstein, B. (2000). Costimulatory effects of interferon-γ and interleukin-1β or tumor necrosis factor-α on the synthesis of Aβ1–40 and Aβ1–42 by human astrocytes. *Neurobiology of Disease, 7*(6 Pt B), 682–689.

Carmeliet, P., & Ruiz de Almodovar, C. (2013). VEGF ligands and receptors implications in neurodevelopment and neurodegeneration. *Cellular and Molecular Life Sciences, 70*(10), 1763–1778.

Carmeliet, P., & Storkebaum, E. (2002). Vascular and neuronal effects of VEGF in the nervous system: Implications for neurological disorders. *Seminars on Cellular and Developmental Biology, 13*(1), 39–53.

Carmeliet, P., Ferreira, V., Breier, G., Pollefeyt, S., Kieckens, L., Gertsenstein, M., et al. (1996). Abnormal blood vessel development and lethality in embryos lacking a single VEGF allele. *Nature, 380*(6573), 435–439.

Chakravarti, B., Chattopadhyay, N., & Brown, E. M. (2012). Signaling through the extracellular calcium-sensing receptor (CaSR). *Advances in Experimental Medicine and Biology, 740*, 103–142.

Chiarini, A., Whitfield, J. F., Bonafini, C., Chakravarthy, B., Armato, U., & Prà, I. D. (2010). Amyloid-β (25-35), an amyloid-β (1-42)

surrogate, and proinflammatory cytokines stimulate VEGF-A secretion by cultured, early passage, normoxic adult human cerebral astrocytes. *Journal of Alzheimer's Disease, 21*(3), 915–926.

Conley, Y. P., Mukherjee, A., Kammerer, C., DeKosky, S. T., Kamboh, M. I., Finegold, D. N., et al. (2009). Evidence supporting a role for the calcium-sensing receptor in Alzheimer disease. *American Journal of Medical Genetics B Neuropsychiatric Genetics, 150B*(5), 703–709.

Dal Prà, I., Chiarini, A., Gui, L., Chakravarthy, B., Pacchiana, R., Gardenal, E., et al. (2014). Do astrocytes collaborate with neurons in spreading the "Infectious" Aβ and tau drivers of Alzheimer's disease? *Neuroscientist*. doi:10.1177/1073858414529828.

Dal Prà, I., Chiarini, A., Nemeth, E. F., Armato, U., & Whitfield, J. F. (2005). Roles of Ca^{2+} and the Ca^{2+}-sensing receptor (CaSR) in the expression of inducible NOS (nitric oxide synthase)-2 and its BH4 (tetrahydrobiopterin)-dependent activation in cytokine-stimulated adult human astrocytes. *Journal of Cellular Biochemistry, 96*(2), 428–438.

Dal Prà, I., Whitfileld, J. F., Pacchiana, R., Bonafini, C., Talacchi, A., Chakravarthy, B., et al. (2011). The amyloid-β_{42} proxy, amyloid-β (25-35), induces normal human cerebral astrocytes to produce amyloid-β_{42}. *Journal of Alzheimer's Disease, 24*(2), 335–347.

Davey, A. E., Leach, K., Valant, C., Conigrave, A. D., & Sexton, A. (2012). Positive and negative allosteric modulators promote biased signaling at the calcium-sensing receptor. *Endocrinology, 153*(3), 4304–4316.

Del Bo, R., Ghezzi, S., Scarpini, E., Bresolin, N., & Comi, G. P. (2009). VEGF genetic variability is associated with increased risk of developing Alzheimer's disease. *Journal of Neurological Sciences, 283*(1–2), 66–68.

Dickerson, B. C., Salat, D. H., Greve, D. N., Chua, E. F., Rand-Giovanetti, E., Rentz, D. M., et al. (2005). Increased hippocampal activation in mild cognitive impairment compared to normal aging and AD. *Neurology, 65*(3), 404–411.

Ewers, M., Sperling, R. A., Klunk, W. E., Weiner, M. W., & Hampel, H. (2011). Neuroimaging markers for the prediction and early diagnosis of Alzheimer's disease dementia. *Trends in Neurosciences, 34*(8), 430–442.

Ferrara, N., Gerber, H. P., & LeCouter, J. (2003). The biology of VEGF and its receptors. *Nature Medicine, 9*(6), 669–676.

Jantaratnotai, N., Ryu, J. K., Schwab, C., McGeer, P. L., & McLarnon, J. G. (2011). Comparison of vascular perturbations in an Aβ-injected animal model and in AD brain. *International Journal of Alzheimer's Disease, 2011*, 918280.

Kaminsky, Y. G., Marlatt, M. W., Smith, M. A., & Kosenko, E. A. (2010). Subcellular and metabolic examination of amyloid-beta peptides in Alzheimer disease pathogenesis: Evidence for Abeta (25–35). *Experimental Neurology, 221*(1), 26–37.

Kawai, M., Kalaria, R. N., Harik, S. I., & Perry, G. (1990). The relationship of amyloid plaques to cerebral capillaries in Alzheimer's disease. *American Journal of Pathology, 137*(6), 1435–1446.

Leach, K., Sexton, P. M., Christopoulos, A., & Conigrave, A. D. (2013). Engendering biased signalling from the calcium-sensing receptor for the pharmacotherapy of diverse disorders. *British Journal of Pharmacology*, Sep 22. doi: 10.1111/bph.12420. [Epub ahead of print].

Logothetis, N. K., & Wandell, B. A. (2004). Interpreting the BOLD signal. *Annual Review of Physiology, 66*, 735–769.

Lu, C., & Mattson, M. P. (2001). Dimethyl sulfoxide suppresses NMDA- and AMPA-induced ion currents and calcium influx and protects against excitotoxic death in hippocampal neurons. *Experimental Neurology, 170*(1), 180–185.

Maillard, M. P., Tedjani, A., Perregaux, C., & Burnier, M. (2009). Calcium-sensing receptors modulate renin release in vivo and in vitro in the rat. *Journal of Hypertension, 27*(10), 1980–1987.

Mattson, M. P. (2007). Calcium and neurodegeneration. *Aging Cell, 6*(3), 337–350.

Mattson, M. P., Cheng, B., Davis, D., Bryant, K., Lieberburg, I., & Rydel, R. E. (1992). Beta-Amyloid peptides destabilize calcium homeostasis and render human cortical neurons vulnerable to excitotoxicity. *Journal of Neurosciences, 12*(2), 376–389.

Merrill, M. J., & Oldfield, E. H. (2005). A reassessment of vascular endothelial growth factor central nervous system pathology. *Journal of Neurosurgery, 103*(5), 853–868.

Meyer, E. P., Ulmann-Schuler, A., Staufenbiel, M., & Krucker, T. (2008). Altered morphology and 3D architecture of brain vasculature in a mouse model for Alzheimer's disease. *Proceedings of the National Academy of Sciences USA, 105*(9), 3587–3592.

Moerke, N. J., & Hoffman, G. R. (2011). Development of in-cell Western assays using far-red fluorophores. *Current Protocols in Chemical Biology, 3*(1), 39–52.

Nemeth, E. F. (2002). The search for calcium receptor antagonists (calcilytics). *Journal of Molecular Endocrinology, 29*(1), 15–21.

Nemeth, E. F., Steffey, M. E., Hammerland, L. G., Hung, B. C., Van Wagenen, B. C., Del Mar, E. G., et al. (1998). Calcimimetics with potent and selective activity on the parathyroid calcium receptor. *Proceedings of the National Academy of Sciences U S A, 95*(7), 4040–4045.

Nygaard, H. B., & Strittmatter, S. M. (2009). Cellular prion protein mediates the toxicity of β-amyloid oligomers: Implications for Alzheimer Disease. *Archives of Neurology, 66*(11), 1325–1328.

Oberheim, N. A., Takano, T., Han, X., He, W., Lin, J. H., Wang, F., et al. (2009). Uniquely hominid features of adult human astrocytes. *Journal of Neurosciences, 29*(10), 3276–3287.

Putcha, D., Brickhouse, M., O'Keefe, K., Sullivan, C., Rentz, D., Marshall, G., et al. (2011). Hippocampal hyperactivation associated with cortical thinning in Alzheimer's disease signature regions in non-demented elderly adults. *Journal of Neurosciences, 31*(48), 17680–17688.

Ruhrberg, C., & Bautch, V. L. (2013). Neurovascular development and links to disease. *Cellular and Molecular Life Sciences, 70*(10), 1675–1684.

Ryu, J. K., & McLarnon, J. G. (2009). A leaky blood-brain barrier, fibrinogen infiltration and microglial reactivity in inflamed Alzheimer's disease brain. *Journal of Cellular and Molecular Medicine, 13*(9A), 2911–2925.

Sanchez, A., Tripathy, D., Luo, J., Yin, X., Martinez, J., & Grammas, P. (2013). Neurovascular unit and the effects of dosage in VEGF toxicity: Role for oxidative stress and thrombin. *Journal of Alzheimer's Disease, 34*(1), 281–291.

Sanchez, A., Wadhwani, S., & Grammas, P. (2010). Multiple neurotrophic effects of VEGF on cultured neurons. *Neuropeptides, 44*(4), 323–331.

Thirumangalakudi, L., Samany, P. G., Owoso, A., Wiskar, B., & Grammas, P. (2006). Angiogenic proteins are expressed by brain blood vessels in Alzheimer's disease. *Journal of Alzheimer's Disease, 10*(1), 111–118.

Tolosa, L., Mir, M., Asensio, V. J., Olmos, G., & Lladó, J. (2008). Vascular endothelial growth factor protects spinal cord motoneurons against glutamate-induced excitotoxicity via phosphatidylinositol 3-kinase. *Journal of Neurochemistry, 105*(4), 1080–1090.

Verkhratsky, A., Butt, A. (2013). 4.6 Functions of Astroglia: 4.6.5 Structural function: astrocytes and the brain-blood barrier. In: *Glial Physiology and Pathophysiology*. 3rd edition. John Wiley & Sons, Chichester, UK. 186–191.

Ward, D. T., & Riccardi, D. (2012). New concepts in calcium-sensing receptor pharmacology and signaling. *British Journal of Pharmacology, 165*(1), 35–48.

Wick, A., Wick, W., Waltenberger, J., Weller, M., Dichgans, J., & Schulz, J. B. (2002). Neuroprotection by hypoxic preconditioning requires sequential activation of vascular endothelial growth factor receptor and Akt. *Journal of Neurosciences, 22*(15), 6401–6407.

Yano, S., Brown, E. M., & Chattopadhyay, N. (2004). Calcium-sensing receptor in the brain. *Cell Calcium, 35*(3), 257–264.

Yassa, M. A., Stark, S. M., Bakker, A., Albert, M. S., Gallagher, M., & Strak, C. E. (2010). High-resolution structural and functional MRI of hippocampal CA3 and dentate gyrus in patients with anamnestic mild cognitive impairment. *Neuroimage, 51*(3), 1241–1252.

Ye, C., Ho-Pao, C. L., Kanazirska, M., Quinn, S., Rogers, K., Seidman, C. E., et al. (1997). Amyloid-beta proteins activate Ca (2+)-permeable channels through calcium-sensing receptors. *Journal of Neuroscience Research, 47*(5), 547–554.

Zand, L., Ryu, J. K., & McLarnon, J. G. (2005). Induction of angiogenesis in the beta–amyloid peptide–injected rat hippocampus. *NeuroReport, 16*(2), 129–132.